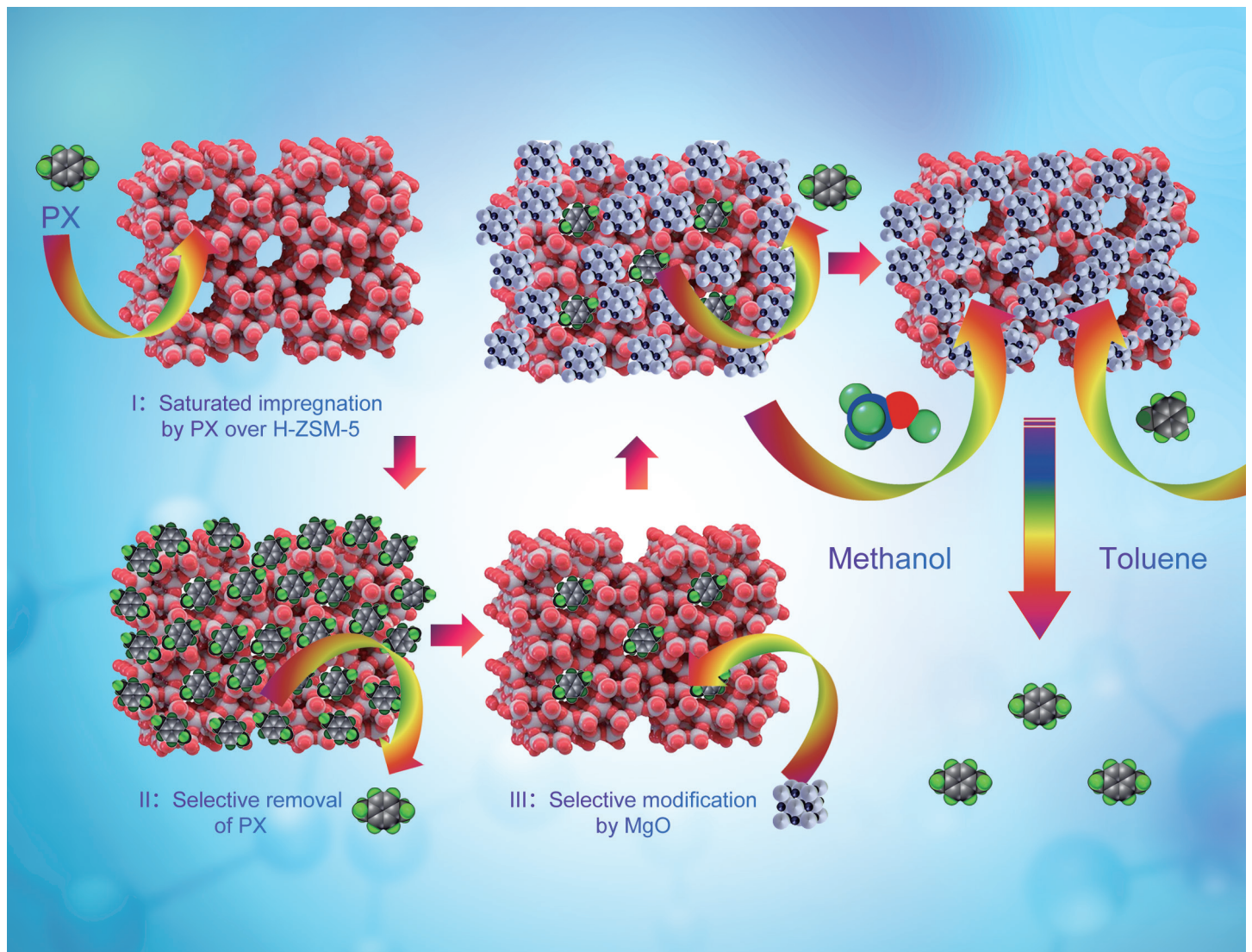


(石油加工)

ACTA PETROLEI SINICA (PETROLEUM PROCESSING SECTION)



ISSN 1001-8719
9 771001 871210



05>

石 油 学 报

(石油加工)

第 37 卷 第 3 期 2021 年 5 月

目 次

研究报告

- 镁选择改性 ZSM-5 催化甲苯甲基化制对二甲苯 * 赵 岩, 马新会, 郑远馨, 夏云生, 任冬梅, 郭新闻(469)
微球型蒽醌加氢钯催化剂的制备和性能 潘智勇(478)
2 种含氧化合物对固载型 Al/Ti 双金属 α -烯烃聚合催化剂及合成 PAO 性能的影响 谭家伦, 姜 豪, 王 丹, 孙 辉, 沈本贤, 刘纪昌(486)
沉淀剂对 CuZnAl 催化剂催化 CO 加氢合成 C_{2+} 醇性能的影响 王竟荣, 高志华, 黄 伟(498)
氮化碳对 Cu-ZnO-Al₂O₃ 催化 CO₂ 加氢合成甲醇的影响 张一凡, 杨文兵, 马清祥, 高新华, 张建利, 李 鹏, 赵天生, 李 蓉(508)
锌改性 HZSM-5 催化正构烷烃临氢芳构化性能 张孔远, 郑传富, 王 崇, 郭宇栋, 刘晨光(518)
高吸附容量吡啶基聚合物刷脱除原油中金属的机理研究 耿 桐, 许 军, 任满年, 曹发海(530)
离子液体 1-己基-4-甲基吡啶四氟硼酸盐与烃类的相互作用规律 史军军, 吴 巍, 蔚 雷(541)
不同氢源对十二烷基芘热裂化反应的影响及作用机理 侯焕娣, 赵 毅, 王子军, 代振宇, 权 奕, 董 明, 龙 军(549)
氢键作用对沥青质超分子聚集的影响 韦胜超, 姚志林, 卞 贺, 阚爱婷, 高智健, 朱丽君, 夏道宏(556)
Al 原子分布对 Y 型分子筛酸强度的影响 叶蔚甄, 任 强, 赵 毅, 代振宇, 王春璐(566)
EVA 加剂量对含沥青质蜡油流变性的改善效果 杨 飞, 陈锦秀, 姚 博, 李传宪, 孙广宇(572)
改性超支化聚乙烯亚胺破乳剂的合成及其应用 张丽锋, 詹宁宁, 陈翠婷, 秦立娟, 赵新星, 滕厚开, 方文军(584)
甲基丙烯酸十二酯-甲基丙烯酸十八酯共聚物的可控合成及其降凝性能 丁丽芹, 冯 豪, 郭 肖, 梁生荣, 李 红(593)
混沌频率电场激励乳化油液滴动力学仿真与响应 龚海峰, 廖治祥, 彭 烨, 邱 值, 余 保, 张贤明, 柳云骐(601)

研究报道

- 不同氧化物对 WO₃/SiO₂ 催化烯烃异构-歧化串联反应的影响 姜伟丽, 籍 星, 郭 岁, 冯 硕, 黎正熙, 孙曼颖, 陈雅琪, 周广林, 周红军(611)
改性 Y 型分子筛吸附脱除模拟油品中氯辛烷 解国应, 宫玉洁, 周东旭, 冯海姣, 王佳烽, 张 晨, 张 伟, 李翠清(619)
液相加氢喷气燃料的贮存安定性能 潘光成, 陈庆岭, 江 磊, 唐乳林, 陶志平(626)
清净剂对柴油雾化液滴空间分布的影响 钟 亮, 朱 民(635)
可逆性吸脱附材料用于气相色谱法测定喷气燃料中芳烃含量 史延强, 徐广通, 常春艳, 张智华, 陶志平(642)
3 种类型石油酸的腐蚀性以及相互影响 葛 霖, 吕 涯, 贾凌燕(653)
催化裂化原料和液相产物中氢含量的回归预测模型 崔守业(662)
EPDM 和 NX8000K 对 iPP 结构及性能的影响 王孟轲, 罗发亮, 尹佳杰, 李 磊, 金政伟(669)
颗粒活性炭对地下水中溶解油的吸附特性 孙 娟, 王 宁, 宋权威, 陈宏坤, 杨晓晴, 郑秀志, 赵朝成, 刘 芳(677)

综述

- 低碳烷烃芳构化反应机理研究进展 吴冰峰, 王子健, 马爱增, 于中伟, 代振宇(690)
有机固体废弃物化学链气化技术研究进展 唐亘炀, 顾 菁, 杨 秋, 黄 振, 袁浩然, 陈 勇(700)
信息

关于《石油学报(石油加工)》网上投稿的特别声明(477); Ei 对中英文摘要的要求(507); 《China Petroleum Processing and Petrochemical Technology》征订启事(634); 《石油学报(石油加工)》征订启事(661); 《石油炼制与化工》征订启事(676)

* 封面文章

期刊基本参数: CN11-2129/TE * 1985 * b * A4 * 250 * zh+en * P * ¥20.00 * 1200 * 26 * 2021-05 本期责任编辑: 赵 敏

ACTA PETROLEI SINICA
(PETROLEUM PROCESSING SECTION)

Vol .37 No .3 May 2021

CONTENTS

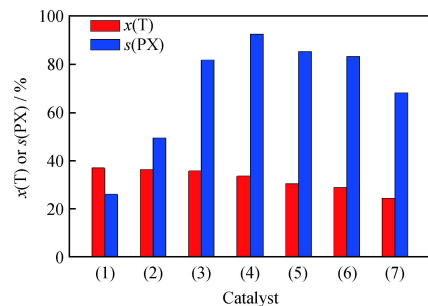
Research Articles

Acta Petrolei Sinica (Petroleum Processing Section), 2021, 37(3): 0469-0477 doi: 10.3969/j.issn.1001-8719.2021.03.001

Selective Toluene Methylation to *p*-Xylene Catalyzed by ZSM-5 Modified With Magnesium Compounds

ZHAO Yan MA Xinhui ZHENG Yuanxin XIA Yunsheng
REN Dongmei GUO Xinwen

In order to improve the *p*-xylene product selectivity without decreasing the activity in toluene methylation , H-ZSM-5 was selectively modified by MgO . Results show that the conversion of toluene and the selectivity of *p*-xylene of MgO-ZSM-5 prepared by *p*-xylene placeholder modification method is much better than those by ordinary impregnation methods .



(1) H-ZSM-5 ; (2) ES-2. 96% MgO-ZSM-5 ; (3) ES-5. 92% MgO-ZSM-5 ;
(4) ES-8. 83% MgO-ZSM-5 ; (5) ESM P-10. 62% MgO-ZSM-5 ;
(6) ATP-11. 04% MgO-ZSM-5 ; (7) NP-11. 78% MgO-ZSM-5

Reaction conditions : $T=460\ ^\circ\text{C}$; $n(\text{T})/n(\text{M})=2/1$;
 $p=0.2\ \text{MPa}$; $\text{MHSV}=2\ \text{h}^{-1}$; $n(\text{H}_2\text{O})/n(\text{T}+\text{M})=n(\text{N}_2)/n(\text{T}+\text{M})=2/1$

Acta Petrolei Sinica (Petroleum Processing Section), 2021, 37(3): 0478-0485 doi: 10.3969/j.issn.1001-8719.2021.03.002

Preparation and Hydrogenation Performance of Microsphere Palladium Catalysts for Anthraquinone Hydrogenation

PAN Zhiyong

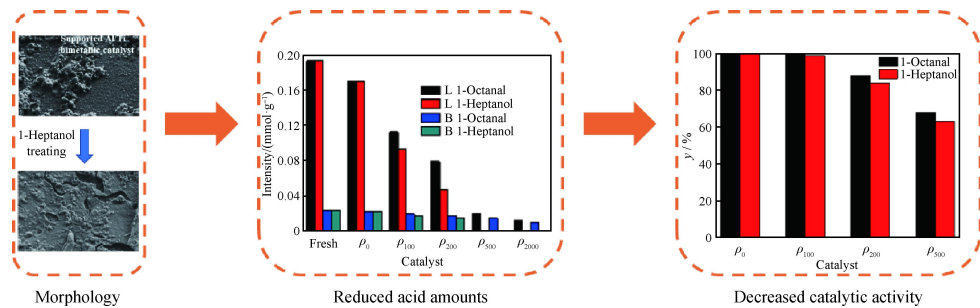
Pd/Al₂O₃ catalyst for anthraquinone hydrogenation in fluidized bed reactor with uniformly distributed Pd was prepared by equal volume impregnation method . With the reaction temperature of 60 °C , the pressure of 0.3 MPa and catalyst mass fraction of 0.27% , the hydrogenation efficiency reaches 10.3 g/L after 15 min .



Effects of Two Oxygenates on Al/Ti-Bimetallic Catalyst for α -Olefin Oligomerization and Properties of Synthesized PAO

TAN Jialun JIANG Hao WANG Dan SUN Hui SHEN Benxian LIU Jichang

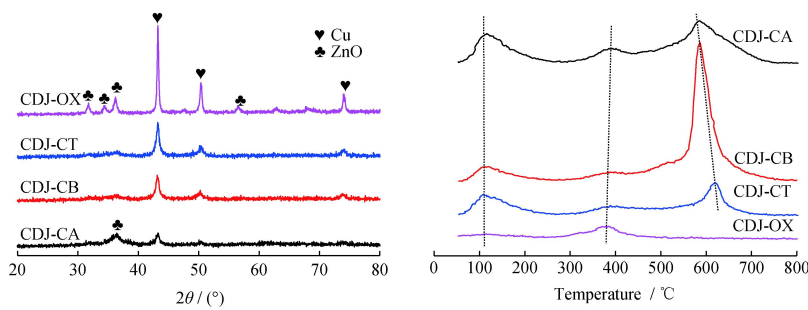
After treatment with 1-heptanol or 1-octanol, the microscopic surface structure of supported Al/Ti-bimetallic catalyst can be changed. This causes reduced amounts of Lewis acid and Brönst acid. Therefore, the oxygenate-treated catalyst shows reduced catalytic activity for PAO synthesis.



Effect of Precipitants on the Performance of CuZnAl Catalyst in CO Hydrogenation to C₂₊ OH

WANG Jingrong GAO Zhihua HUANG Wei

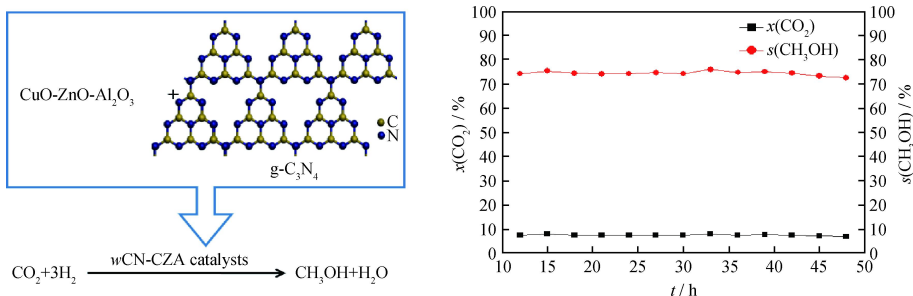
Precipitators determine the structure of catalyst. And Cu species in high dispersion state are more conducive to the improvement of catalyst activity, while an appropriate proportion of surface weak and medium strong base sites is in favor of the formation of C₂₊ OH.



Effect of Carbon Nitride Addition on Cu-ZnO-Al₂O₃ Catalytic Performance for CO₂ Hydrogenation to Methanol

ZHANG Yifan YANG Wenbing MA Qingxiang GAO Xinhua ZHANG Jianli LI Peng ZHAO Tiansheng LI Rong

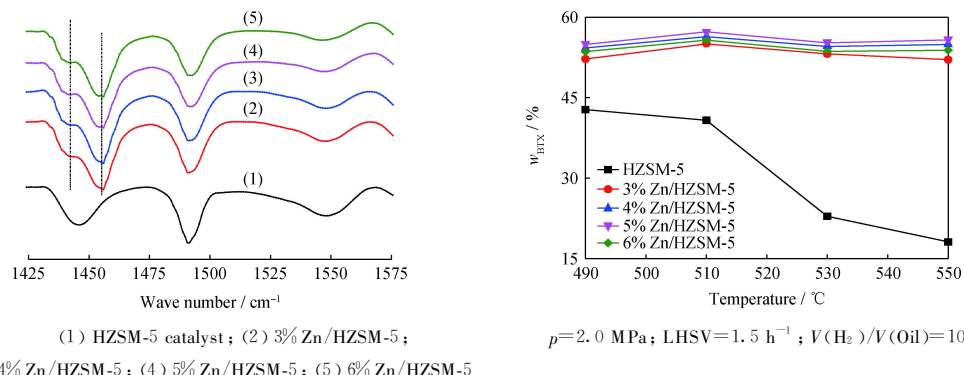
Catalytic performance of wCN-CZA catalysts for methanol synthesis from CO₂ hydrogenation is significantly impacted by g-C₃N₄ content. With 5% mass fraction g-C₃N₄ in the catalyst, optimum methanol production can be obtained. g-C₃N₄ addition can improve copper active species dispersion and increase medium-strong base sites in the catalyst. Both of them can improve methanol synthesis from CO₂ and H₂.



Catalytic Performance of Zn Modified HZSM-5 Catalyst in n-Alkane Hydroaromatization

ZHANG Kongyuan ZHENG Chuanfu WANG Chong GUO Yudong LIU Chengguang

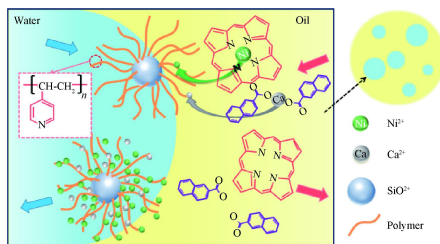
A series of Zn/HZSM-5 catalysts with different ZnO loading contents were prepared by the equal volume impregnation method. Results show that Zn modification can adjust the acid properties of the HZSM-5 catalyst and the selectivity of BTX firstly increases and then decreasing with the increases of ZnO loading content. Moreover, the highest catalytic performance is obtained when ZnO loading mass fraction is 5%.



Study on Crude Oil Metal Removal Mechanism of Pyridine Polymer Brush With High Absorption Capacity

GENG Tong XU Jun REN Mannian CAO Fahai

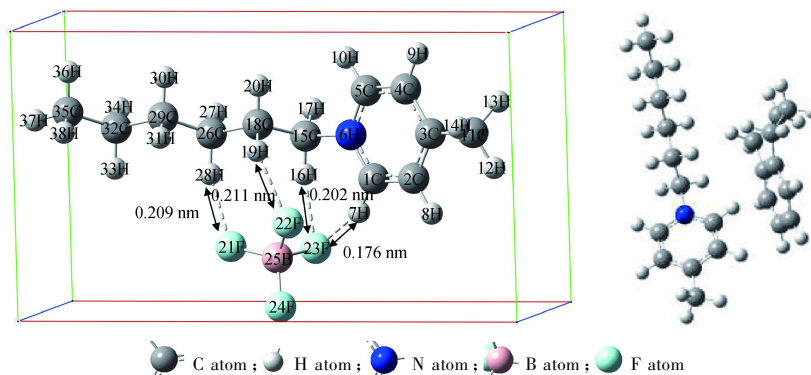
Pyridine based polymer brush ($\text{P4VP}@\text{SiO}_2$) was prepared for nickel and calcium removal from crude oils. Due to high density pyridine groups in the inner layer of spherical polymer brush, $\text{P4VP}@\text{SiO}_2$ exhibits excellent absorption capacity for both nickel and calcium. Nickel and calcium removal ratios can be 68.4% and 62.2%, respectively.



Interaction Mechanism Between $[\text{C}_6\text{MPy}] [\text{BF}_4^-]$ Ionic Liquid and Hydrocarbons

SHI Junjun WU Wei XI Lei

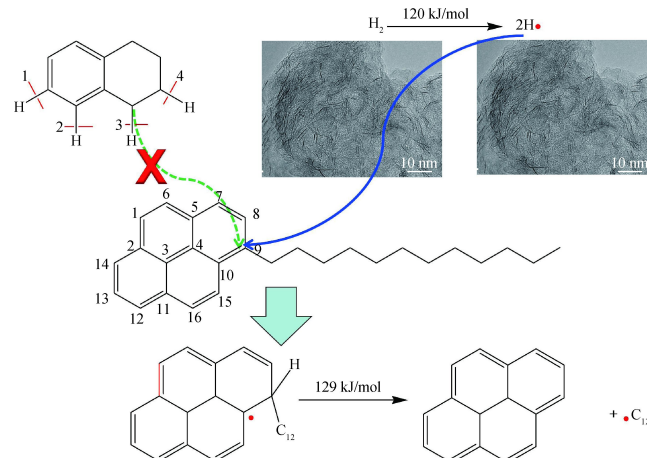
The dominant force between $[\text{C}_6\text{MPy}] [\text{BF}_4^-]$ and aromatic molecules is found to be the C—H— π interactions between cations of $[\text{C}_6\text{MPy}] [\text{BF}_4^-]$ and the aromatic ring. The strength of the C—H— π interaction is related to the conjugation π bond delocalization degree of aromatics, and weakens the hydrogen bonding between cations and anions.



Effects and Mechanisms of Different Hydrogen Sources on Dodecyl Pyrene Thermal Cracking Reactions

HOU Huandi ZHAO Yi WANG Zijun DAI Zhenyu QUAN Yi DONG Ming LONG Jun

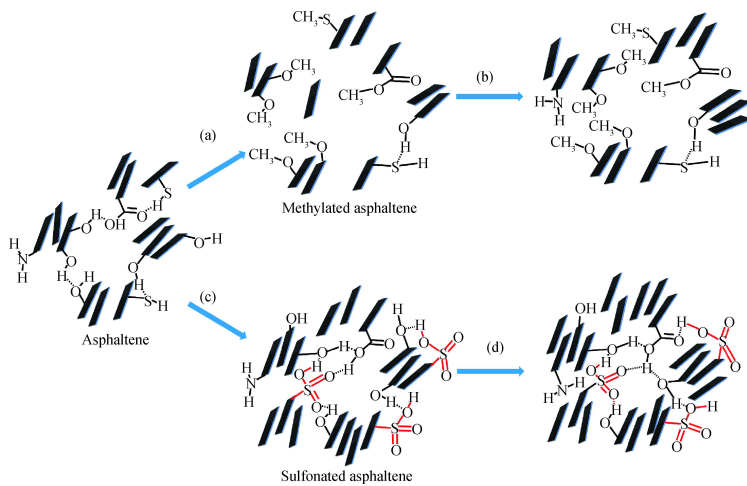
Hydrogen radicals generated by the dispersed catalyst activation can be easily attached on the *Ipo*-carbon position in dodecyl pyrene. Thus, cracking barrier of the alpha C=C bond in the side chain can be significantly reduced and easily broken. Although THN can provide α position hydrogen, there is a large steric hindrance between α position hydrogen in THN and *Ipo*-carbon in dodecyl pyrene. Therefore, α position hydrogen in THN can't provide directional hydrogenation and improve cracking reactions. The main function of THN is to stabilize the free radicals and inhibit free radical propagation reaction.



Effects of Hydrogen Bonding Interactions on the Asphaltene Supramolecular Aggregation

WEI Shengchao YAO Zhilin BIAN He KAN Aiting GAO Zhijian ZHU Lijun XIA Daohong

By studying the effect of methylation, carboxylation and sulfonation on the asphaltenes structures and aggregation, the mechanism of hydrogen bonding affecting asphaltene aggregates has been proposed, in which the introduction of methyl inhibits the asphaltene aggregation, while the introduction polar functional groups (e.g., carboxyl and sulfonic acid group) promotes the aggregation.

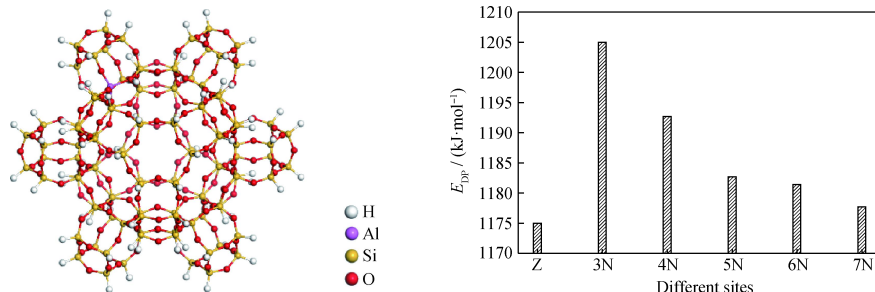


(a) Methylation; (b) Re-aggregation; (c) Sulfonation; (d) Re-aggregation

Effects of Al Atom Distribution on Acid Strength of Y Zeolite

YE Weizhen REN Qiang ZHAO Yi DAI Zhenyu WANG Chunlu

The effect of Al atom distribution on acid strength of Y zeolite was studied, the results show that the acid strength of Y zeolite decreases when Al atoms locate at NNN and NNNN positions, and the effect on acid strength of Y zeolite is negligible when Al atoms locate at further positions.

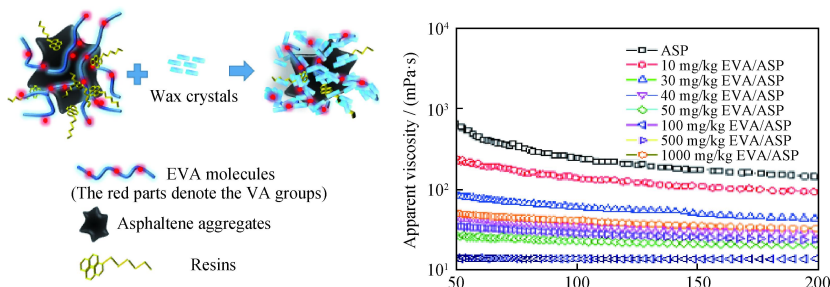


Z : The initial Y zeolite cluster model ; E_{DP} : The energy required to remove one H^+ from the zeolite , indicating the acid strength of the zeolite ; 3N—7N : Positions of Al atom

Effects of EVA Additive Dosage on Rheological Properties of Asphaltenic Waxy Oils

YANG Fei CHEN Jinxiu YAO Bo LI Chuanxian SUN Guangyu

Additive EVA can adsorb on the surface of associated asphaltenic colloidal particles to form EVA-asphaltene composite particles, which can demonstrate synergistic effect on improving rheological property of waxy oils. It was observed that, with increasing EVA mass fraction, this synergistic effect is good at the beginning but become bad later.

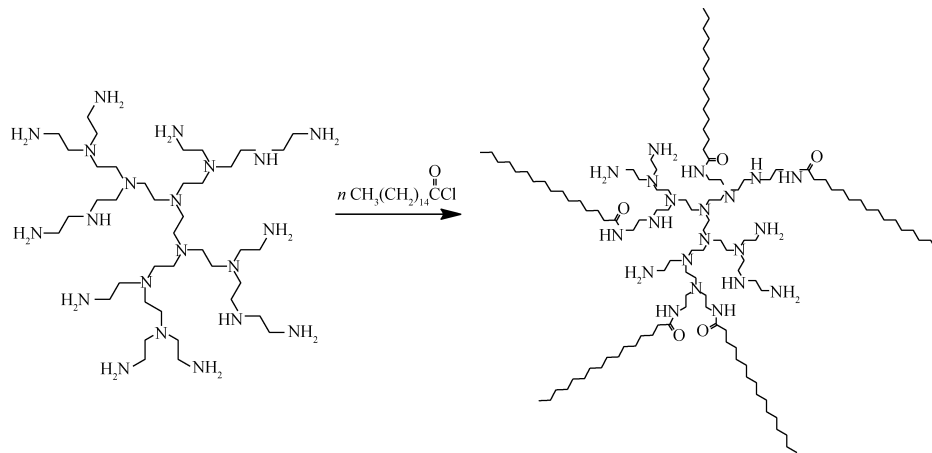


With the increase of EVA mass fraction,rheological property of waxy oil gets better and then gets worse

Synthesis of Modified Hyperbranched Polyethyleneimine and Its Application in Demulsification

ZHANG Lifeng ZHAN Ningning CHEN Cuiting QIN Lijuan ZHAO Xinxing TENG Houkai FANG Wenjun

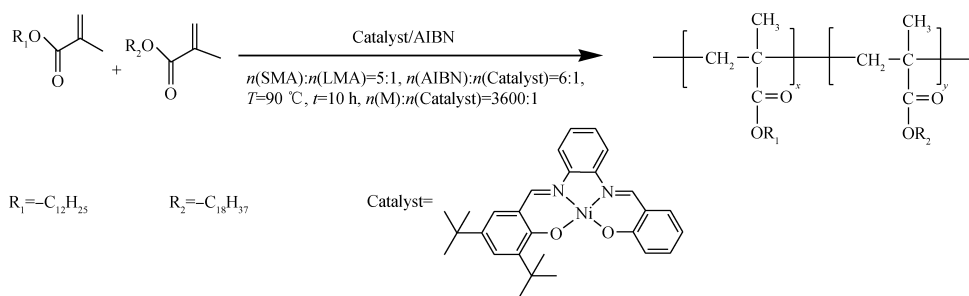
HPEI-C₁₆ was developed to meet the requirements of the O/W emulsion demulsification. Due to the specific highly branched structure, the demulsifier rapidly destroys the interface film and causes large oil droplets to aggregate. Then, oil-water separation arises in the emulsion due to gravity action.



Controllable Synthesis of Lauryl Methacrylate-Stearyl Methyl Acrylate Copolymer and Its Pour Point Depression Performance

DING Liqin FEGN Hao GUO Xiao LIANG Shengrong LI Hong

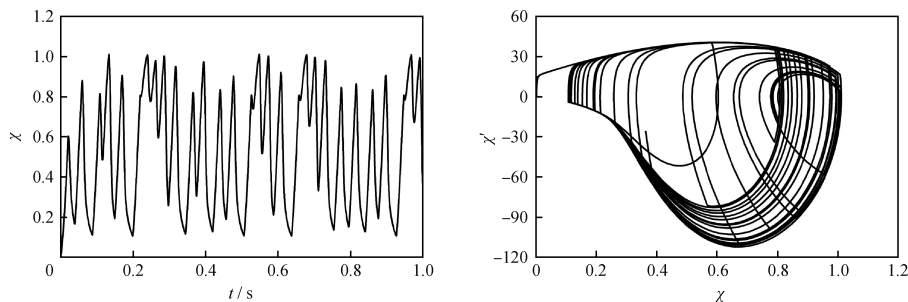
Poly (lauryl methacrylate-stearyl methyl acrylate) (PHMA) was controllably synthesized with Salen-Ni-Salicylaldehyde/azodiisobutyronitrile (AIBN) catalyst system. For Salen-Ni-Salicylaldehyde, catalyst activity is $11.035 \times 10^4 \text{ g}/(\text{mol} \cdot \text{h})$. The synthesized copolymer M_n is from 0.864×10^5 to 2.532×10^5 . With adding the above copolymer, either the pour point of diesel fraction (300–340 °C) or lubricant fractions (380–400 °C) can be decreased. When 0.5% mass fraction copolymer was added to the lubricant fraction (380–400 °C), the pour point depression has the best effect ($\Delta T_{SP} = 15 \text{ }^\circ\text{C}$). It was also found that pour point depression of copolymer is better than that of blend polymer.



Dynamic Simulation and Response of Emulsion Droplets Excited by Chaotic Frequency Electric Field

GONG Haifeng LIAO Zhixiang PENG Ye QIU Zhi YU Bao ZHANG Xianming LIU Yunqi

The chaotic frequency pulse electric field is constructed by using the Chaotic-Pulse-Position Modulation method, which has the best pulse width to excite the droplet chaotic vibration. The droplet gets a large amount of tensile deformation at high frequency, but relatively small and stable at low frequency.

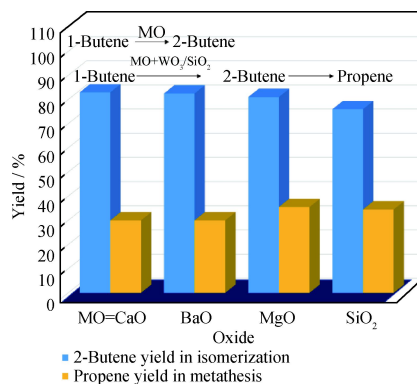


Research Notes

Effect of Different Oxides on Olefin Isomerization-Metathesis Catalyzed by WO_3/SiO_2 Catalyst

JIANG Weili JI Xing GUO Wei FENG Shuo LI Zhengxi SUN Manying CHEN Yaqi ZHOU Guanglin
ZHOU Hongjun

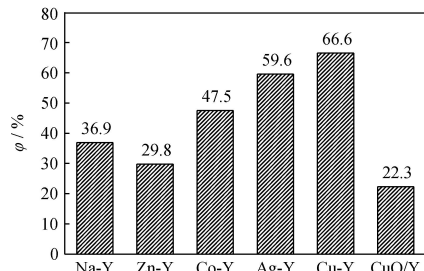
It is found that MgO shows the best promoting effect on the isomerization-metathesis tandem reaction of 1-butene to produce propene catalyzed by WO_3/SiO_2 , although its butene isomerization function is not the best.



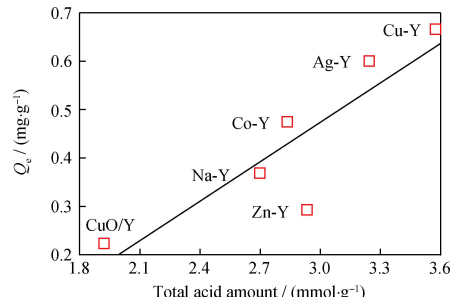
Adsorption of 1-Chlorooctane in Model Oil Using Modified Y Zeolite

XIE Guoying GONG Yujie ZHOU Dongxu FENG Haijiao WANG Jiafeng ZHANG Chen ZHANG Wei LI Cuiqing

The acidity of modified Y zeolite plays a very important role on its adsorption capacity for 1-chlorooctane. And high total acid amount of Y zeolite favors the increase of adsorption capacity.



φ —The removal rate of chlorine

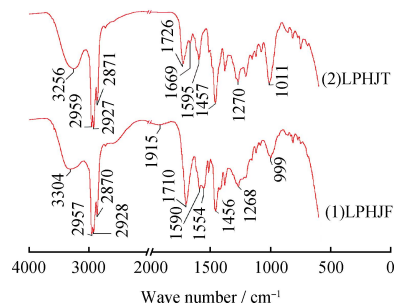


Q_e —The adsorptive capacity of chlorine

Storage Stability of Liquid-Phase Hydrogenating Jet Fuels

PAN Guangcheng CHEN Qingling JIANG Lei TANG Rulin TAO Zhiping

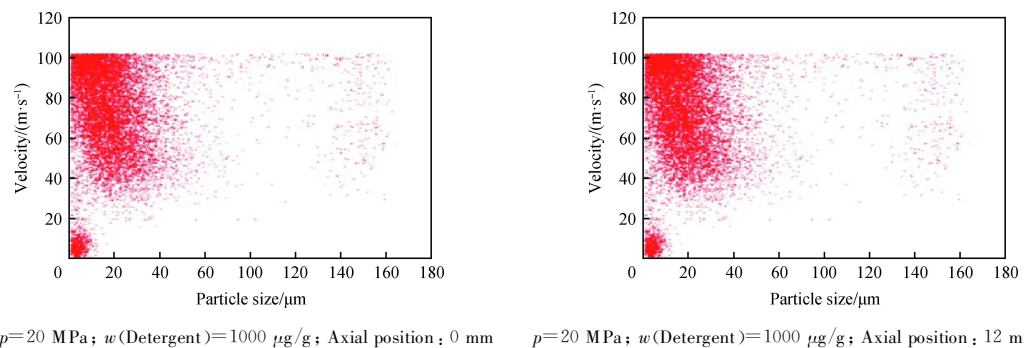
Storage stability of the liquid-phase hydrogenating jet fuels was invested according to the No.3 jet fuel national standard. The unstable components show significant negative effects on the thermal stability of liquid-phase hydrogenating jet fuels during storage, which are mainly phenol, carboxylic acid or ketone, heavy aromatics and polymers, etc., except for a small amount of sulfur-containing and nitrogen-containing compounds.



Effects of Detergents on the Spatial Distribution of Diesel Atomizing Droplets

ZHONG Liang ZHU Min

The law of distribution of diesel atomization under detergents was investigated by PDA. The results show that detergents could improve the capabilities of diesel atomization droplets under different pressures, and the attenuation of droplets with detergents is faster than that of droplets without detergents at far positions from nozzle.

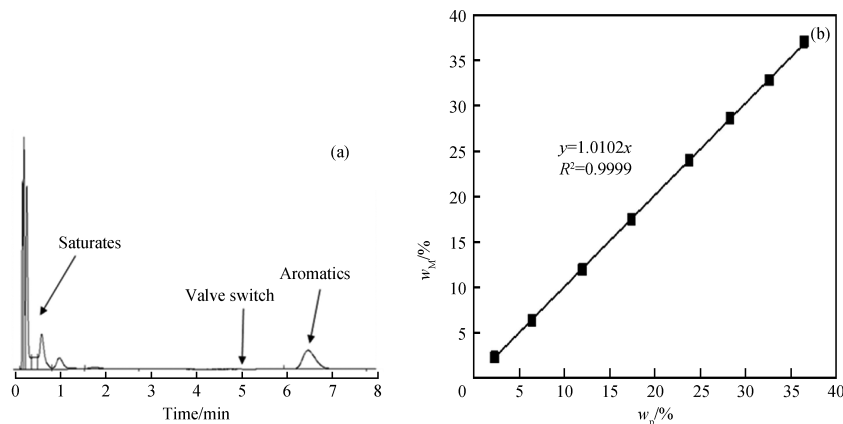


$p=20 \text{ MPa}$; $w(\text{Detergent})=1000 \mu\text{g/g}$; Axial position: 0 mm $p=20 \text{ MPa}$; $w(\text{Detergent})=1000 \mu\text{g/g}$; Axial position: 12 mm

Determination of Aromatics in Jet Fuel by Gas Chromatography With Reversible Adsorption-Desorption Materials

SHI Yanqiang XU Guangtong CHANG Chunyan ZHANG Zhihua TAO Zhiping

Gas chromatography (GC) with column packed with reversible adsorption-desorption materials for aromatics was used to analyze total aromatics in jet fuel. The accuracy and repeatability of GC method can satisfy the requirement of jet fuel quality control. The proposed GC method can significantly improve analysis efficiency.

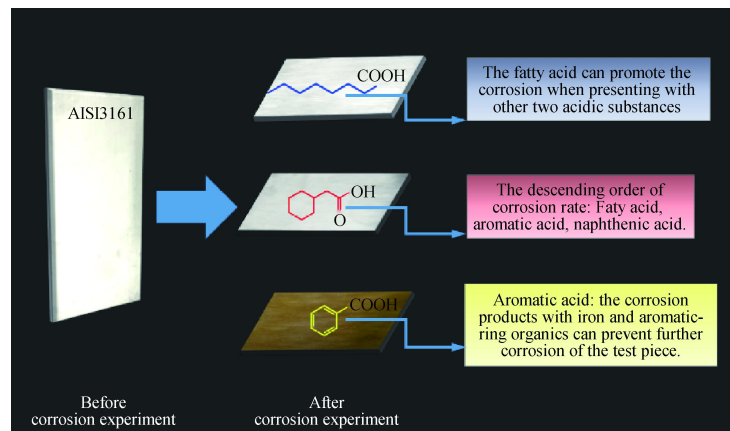


(a) Separation chromatogram of saturates and aromatics in jet fuel;

(b) Linear correlation between measured aromatic mass fraction (w_M) and prepared aromatics standard mass fraction (w_P) in sample No. 8—15

Corrosivity and Interactions of Different Acidic Species in Petroleum Fractions

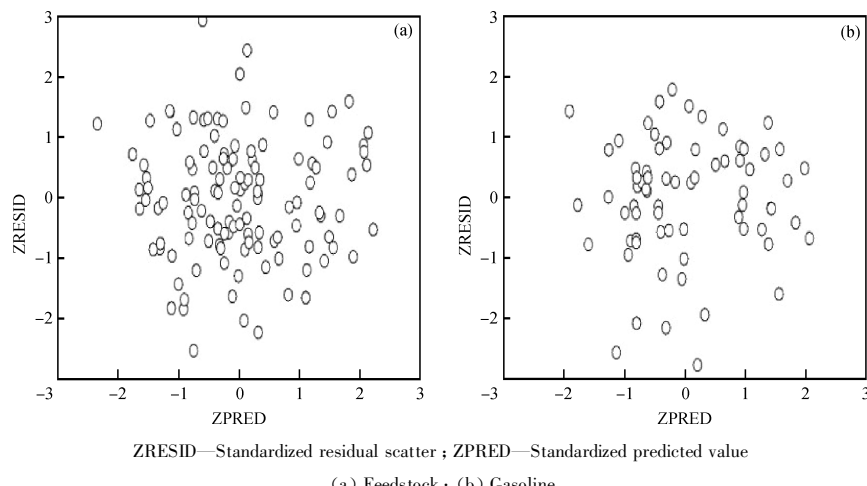
GE Lin LU Ya JIA Lingyan



Regression Model of FCC Feedstock and Liquid Products Hydrogen Content

CUI Shouye

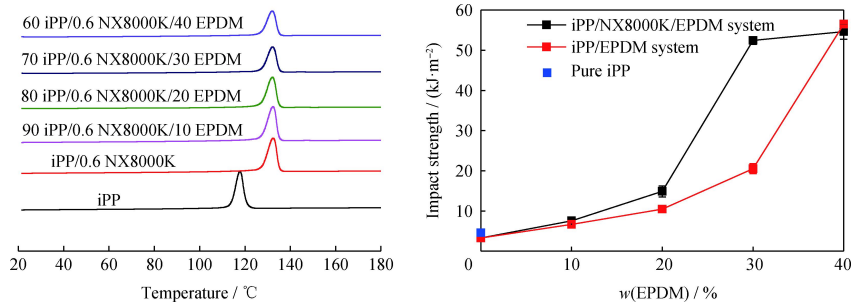
The standardized residual of the regression are independent on the variable value level , and there are almost no outliers , indicating that the regression models are relatively ideal . The constructed model could be used to predict the hydrogen mass fraction of FCC feedstock and liquid products quickly and effectively .



Effects of EPDM and NX8000K on the iPP Structure and Performance

WANG Mengke LUO Faliang YIN Jiajie LI Lei JIN Zhengwei

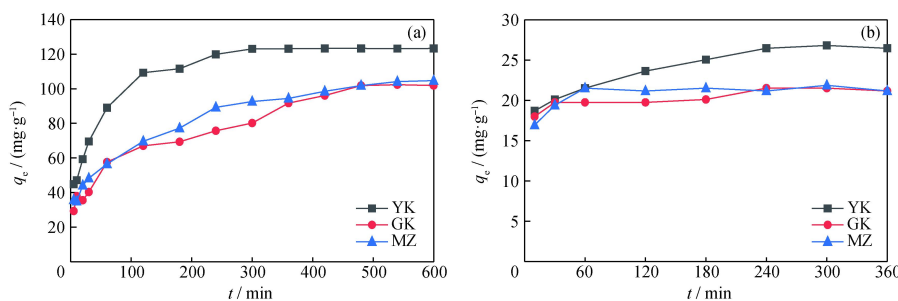
When the NX8000K mass fraction is 0.6% and EPDM has a higher mass fraction being 40%, the crystallization temperature of iPP/EPDM/NX8000K still reaches 132.0 °C, and the relative crystallinity is 53.5%. Moreover, when EPDM mass fraction is 30%, the impact strength of iPP/EPDM/NX8000K reaches 52.4 kJ/m², which is 2.6 times of the corresponding iPP/EPDM binary blend.



Adsorption Characteristics of Dissolved Oil on Granular Activated Carbon in Groundwater

SUN Juan WANG Ning SONG Quanwei CHEN Hongkun YANG Xiaoqing ZHENG Xiuzhi ZHAO Chaocheng LIU Fang

The adsorption process of 40–60 mesh coconut shell activated carbon for dissolved diesel oil and crude oil in groundwater follows Lagergren pseudo second order kinetic equation. Salinity has little effects on the adsorption of dissolved oil, and the optimal pH value and temperature are 7 and 25 °C respectively.



(a) $0^\#$ diesel oil, m (Activated carbon)=0.1 g; (b) Venezuelan crude oil, m (Activated carbon)=0.015 g

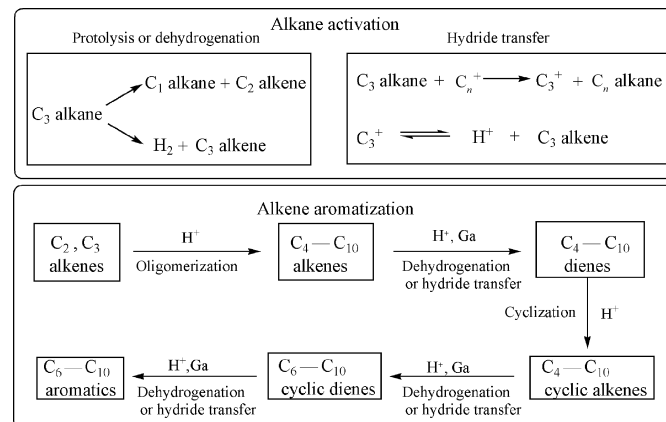
V (Groundwater)=100 mL; $T=20$ °C; $r=135$ r/min; Particle size of activated carbon: 40–60 mesh;

The initial mass fractions of diesel oil and crude oil are 123.70 and 4.67 mg/L, respectively.

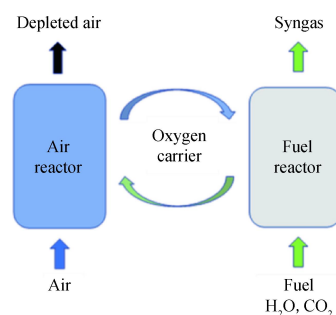
Research Progress in the Mechanism of Light Alkane Aromatization

WU Bingfeng WANG Zijian MA Aizeng YU Zhongwei DAI Zhenyu

The pathways of light hydrocarbon aromatization can be divided into alkane activation and alkene aromatization. During alkane activation, alkanes are converted to alkene by protolysis, dehydrogenation or hydride transfer reaction. Then, alkenes are finally converted into aromatics through oligomerization, cyclization, cyclization and other reactions.

**Research Progress in Chemical Looping Gasification Technology of Organic Solid Waste**TANG Genyang GU Jing YANG Qiu HUANG Zhen
YUAN Haoran CHEN Yong

The combination of chemical looping gasification (CLG) with organic solid waste treatment enriched the means of organic solid waste resource and energy utilization. This article takes the types of organic solid wastes, oxygen carriers (OC) types and reaction devices as examples to systematically summarize the current status of CLG treatment of organic solid wastes, and prospects for its future research directions.



特约英文编审：范志明，加拿大不列颠哥伦比亚大学化学及生物工程博士，先后在加拿大自然资源部及加拿大国家研究院工作，现供职BP美国公司，研究领域包括重质油加工、石油加工过程中沥青质沉淀及石油化学等。

刘磊，中国科学院过程工程研究所“百人计划”研究员，博士生导师。迄今在 *J. Am. Chem. Soc.*, *Angew. Chem. Int. Ed.* 和 *ACS Catal.* 等期刊发表论文 40 余篇。

夏长久，博士，现供职中国石油化工科学研究院，研究领域包括杂原子分子筛催化材料与烃类选择性催化氧化。